Copper nanoparticles stabilized with cashew gum: Antimicrobial activity and cytotoxicity against 4T1 mouse mammary tumor cell line

Adriany Amorim[1], Ana Carolina Mafud[2], Silvania Nogueira[1],
Joilson Ramos- Jesus[1], Alyne Rodrigues de Araújo[1],
Alexandra Plácido[3,4], Maria Brito Neta[5],
Michel Muálem Moraes Alves[6],
Fernando Aécio Amorim Carvalho[6],
Daniel Dias Rufino Arcanjo[1,6] ⓘD, Sacha Braun[5],
Marta Sánchez-Paniagua López[7], Beatriz López-Ruiz[7],
Cristina Delerue-Matos[8], Yvonne Mascarenhas[2],
Durcilene Silva[1], Peter Eaton[1,9] and
José Roberto Souza Almeida Leite[10]

Abstract
Copper nanoparticles stabilized with cashew (CG-CuNPs) were synthesized by reduction reaction using ascorbic acid and sodium borohydride, using the cashew gum (CG) as a natural polymer stabilizer. Dynamic light scattering, atomic force microscopy, Fourier-transform infrared spectroscopy, UV-Vis spectrophotometry, and x-ray diffraction were used to characterize the nanoparticles (CG-CuNPs), and copper was quantified by electrochemical measurement. The UV-vis spectra of the CG-CuNPs confirmed the formation of nanoparticles by appearance of a surface plasmon band at 580 nm after 24 h of reaction. The Fourier-transform infrared spectrum of CG-CuNPs showed the peak at 1704 cm^{-1} from cashew gum, confirming the presence of the gum in the nanoparticles. The average size of CG-CuNPs by dynamic light scattering and atomic force microscopy was around 10 nm, indicating small, approximately spherical particles. Antimicrobial assays showed that CG-CuNPs had activity against *Staphylococcus aureus* ATCC 29213 with a minimal inhibitory concentration of 0.64 mM. The cytotoxicity assay on BALB/c murine macrophages showed lower cytotoxic effects for CG-CuNPs than $CuSO_4 \cdot 5H_2O$. Viability cell assays for CG-CuNPs at (0.250 mM) inhibited by 70% the growth of 4T1 LUC (4T1 mouse mammary tumor cell line) and NIH 3T3 cells (murine fibroblast cells) over a 24-h period. Therefore, CG-CuNPs can be used as an antimicrobial agent with lower cytotoxic effects than the $CuSO_4 \cdot 5H_2O$ precursor.

Keywords
Copper nanoparticles, cashew gum, cancer, antimicrobial

[1]Centre for Biodiversity Research and Biotechnology, Biotec, Universidade Federal do Piaui, Parnaíba 64202020, PI, Brazil
[2]São Carlos Physical Institute, University of São Paulo, USP, São Carlos 13566590, SP, Brazil
[3]Glial Cell Biology Lab, Instituto de Investigação e Inovação em Saúde, Universidade do Porto, Porto 4200135, Portugal
[4]Bioprospectum, Lda, UPTEC, Porto 4200135, Portugal
[5]Department of Genetics and Morphology, Institute of Biology Science, University of Brasilia, Brasília-DF 70910900, Brazil
[6]Medicinal Plants Research Center, NPPM, UFPI, Teresina 64049550, PI, Brazil
[7]Departamento de Química en Ciencias Farmacéuticas, Facultad de Farmacia, Universidad Complutense de Madrid, Ciudad Universitaria, Madrid 28240, Spain

[8]REQUIMTE/LAQV, Superior Engineering Institute of Porto, Polytechnic Institute of Porto, Porto 4200072, Portugal
[9]Requimte/LAQV, Departamento de Química e Bioquímica, Faculdade de Ciências da Universidade do Porto, Rua do Campo Alegre 687, Porto 4169007, Portugal
[10]Nucleo de Pesquisa em Morfologia e Imunologia Aplicada, NuPMIA, Area Morphology, Faculty of Medicine, University of Brasília, UnB, 70910900, Campus Darcy Ribeiro, Brasília, Brazil

Corresponding author:
José Roberto Souza Almeida Leite, Nucleo de Pesquisa em Morfologia e Imunologia Aplicada, NuPMIA, Area Morphology, Faculty of Medicine, Universidade de Brasília, Faculdade de Medicina, Campus Universitário Darcy Ribeiro 70910900, Brasilla.
Email: jrsaleite@gmail.com

Introduction

Copper-based materials are widely used since copper has excellent electrical conductivity, good catalytic behavior, relatively low costs, and plays a significant role in modern electronic circuits.[1] Thus, copper nanoparticles (NPS) have drawn the attention of scientists as having potential for use as an essential component in future nano-devices.

Along with NPs composed of other metals, the recent interest in CuNPs is propelled by the advances of NPs as a cheap alternative for use in the area of micro-electronics applications as well as the possibility of using them as novel antimicrobial and anticancer agents.[2] Researchers have also recommended the use of metallic NPs as disinfectants for wastewater generated by hospitals containing some infectious microorganisms such as strains of *Escherichia coli* (MTCC: 443, 739, 1302, 1687) and of *Staphylococcus aureus* (NCIM: 2079, 5021, 5022).[3] However, copper, or copper oxide NPs are much more toxic than other metallic NPs, such as those composed of silver and titanium, and their toxicity is attributed to the release of copper ions inside cells, on the other hand, the toxicity of copper oxide is less than the toxicity of copper sulfate.[3,4]

Cashew gum (CG) is a natural product which is extracted in a sustainable manner and at low cost, derived from the exudate of the cashew tree (*Anacardium occidentale*), native to, and distributed widely in northeastern Brazil.[5] Chemically, CG is a non-toxic complex polysaccharide composed of mainly (72–73%) β-D-galactose, with main chains of β-D-galactose 1→3 linked with side chains of galactose and glucose, and also α-D-glucose (11–14%), α-D-arabinose (4.6–5%), α-D-rhamnose (3.2–4%), and α-D-glucuronic acid (4.7–6.3%),[6–8] which may act as a stabilizing agent of NPs by steric or electrostatic effects.[9,10]

On the basis of the finding that the antibiotic resistance is one of the biggest public health challenges of our time[11] and that the global cancer burden is estimated to have risen to 18.1 million new cases and 9.6 million deaths in 2018,[12] the objectives of this work were the preparation and physicochemical characterization of copper NPs stabilized with the natural polymer CG to investigate antimicrobial activity and cytotoxicity against normal and tumor cells.

Materials and methods

Reagents

Copper sulfate pentahydrate P.A. ($CuSO_4·5H_2O$), ascorbic acid 99%, sodium borohydride ($NaBH_4$ $\geq$98%), nitric acid (65%), and mercuric chloride ($HgCl_2$ 99.5%) were purchased from Sigma-Aldrich (Saint Louis, MO) and used as received. CG was isolated according to the method described by Castro et al.[13] Water used in all experiments was purified with a Milli-Q Ultrapure system (Millipore). 3-[4,5-Dimethylthiazol-2-yl]-2,5-diphenyltetrazolium bromide (MTT) and RPMI 1640 medium were purchased from Sigma-Aldrich.

Synthesis of CG-CuNPs

Copper NPs were synthesized by the chemical reduction of $CuSO_4·5H_2O$ with ascorbic acid, sodium borohydride, and CG in suspension. A 0.5% CG was dispersed in water by stirring for 24 h. The initial concentrations were 10 mM for $CuSO_4·5H_2O$ and 0.5% CG at a 1:1 ratio (solution 1). Meanwhile, solution 2 consisted of 30% ascorbic acid and freshly prepared 1M sodium borohydride (at a 1:1 ratio). The two solutions were rapidly mixed in the ratio of 25:3 parts (solution 1: solution 2). The reduction then occurred over 72 h of stirring at 600 r/min in a water bath at 50°C. After 24, 48, and 72 h, aliquots for UV-Vis analysis were removed. The final product was stored under refrigeration for further characterization.

UV-Vis

UV-vis absorption spectra of CG-CuNPs were acquired using a UV-1800 Shimadzu Spectrophotometer (Shimadzu Corporation, Kyoto, Japan). All measurements were performed at 25°C and samples were diluted 1:200 in water.

DLS and zeta potential

Dynamic light scattering (DLS) from distribution measurements and zeta potential of copper NPs in solution were performed in a Zetasizer Nano-ZS90 (Malvern Instruments, UK), using laser diffraction to measure the particle size of suspensions with equilibration for 2 min to 25°C before the measurements. Three measurements per sample were made and the result was expressed as the mean $\pm$ SD.

Electrochemical measurements

The three-electrode system was composed of a glassy carbon working electrode (GCE; $\Phi = 2$ mm, used for differential pulse voltammetry (DPV) measurement), an Ag/AgCl reference electrode, and a platinum wire counter electrode. CG-CuNPs (25 μL) were immersed in 22.5 mL of 100 mM HNO_3 under stirring for 5 min. To this solution 2.5 mL 10 mM $Hg(NO_3)_2$ was added. DPV was used to detect the dissolved Cu^{2+} in solution.

For this, an in situ preparation of mercury film on a GCE with a deposition time of 120 s and deposition potential of -0.8 V was used. After 30 s rest time, the anodic stripping voltammogram was scanned over a potential range from -0.3 to $+0.2$ V and the anodic peak current $i_{p,a}$ of copper appeared at -0.05 V was taken as the analytical response. The following DPV conditions were selected: increment $E = 0.01$ V, amplitude $= 0.05$ V, pulse width $= 0.06$ s, sample width $= 0.02$ s, pulse period $= 0.2$ s. Electrochemical measurements were performed with an Autolab potentiostat (PGSTAT 10) using the general purpose electrochemical system (GPES) software.

FTIR-ATR spectroscopy

The identification of CG-CuNPs was investigated by Fourier-transform infrared spectroscopy (FTIR) using a Thermo Nicolet 6700 spectrometer (Thermo Scientific Inc., MA) with the attenuated total reflection (ATR) technique in the spectral range from 4000 to 400 cm^{-1}. The powdered sample was placed onto the ATR crystal and the sample spectrum was collected. The spectrum from CG-CuNPs was compared to that of purified CG.

X-ray diffraction

X-ray diffraction (XRD) was carried out on dried samples in order to determine the phase, percentage of crystallinity, and crystallite size of the copper present in the NPs. The experiment was performed with a diffractometer (Rigaku Ultima IV, Spring, TX) using CuKα monochromatic radiation in step-scanning mode ($0.02°$ step) over the range of 8–$60°$ with an exposure time of 5 s/step. Further investigations were conducted applying the Rietveld refinement, in order to fit the starting model of the phases, found by searching the previous phase, to the entire powder pattern obtained from the experiment, using the software MAUD. The structures were designed using HyperChem and geometrically optimized using model building in the software (HyperChem Professional 8.0.6 (Hypercube Inc., Gainesville, FL).

Atomic force microscopy (AFM)

Samples for AFM were prepared by depositing a 10-μL of CG-CuNPs (diluted 1:10 in Milli-Q water) solution on freshly cleaved mica at room temperature. After 5 min the sample was washed three times with water and finally dried at room temperature. Imaging was carried out with AFM model TT-AFM (AFM Workshop, USA) in vibrating mode. Cantilevers (ACT-20) with a resonant frequency of around 300 kHz and nominal tip radius <10 nm (ACT, AppNano, USA) were used. Images were analyzed using Gwyddion 2.4 software and the average size of copper NPs was expressed as the mean $\pm$ SD. Representative AFM height images at 512×512 pixels resolution are shown here.

Microbiological assay

Antimicrobial activity of CG-CuNPs was tested in vitro using a standard strain of *S. aureus* (ATCC 29213). The minimal inhibitory concentration (MIC) was examined by serial microdilution method in 96-well plates using Mueller-Hinton broth (DIFCO^{TM}) according to the methods described by the Clinical & Laboratory Standards Institute.[14] The tested concentrations ranged from 0.08 to 2.50 mM of copper. The final inoculum of all studied organisms was 5×10^5 colony forming units/mL (CFU mL^{-1}). MIC was read after 24 h of incubation at $35 \pm 2°$C. Minimal bactericidal concentration (MBC) was determined after 24 h of incubation at $35 \pm 2°$C of the aliquots (10 μL) from all wells with concentrations equal or higher to the MIC. Oxacillin was used as the standard antimicrobial compound (positive control) and all assays were performed in triplicate.

Cytotoxicity assessment

MTT assay. The cytotoxicity of CG-CuNPs and CuSO$_4\cdot$5H$_2$O was evaluated using the MTT assay in murine macrophages obtained from the peritoneal cavity of three BALB/c mice, according to Rodrigues et al.,[15] with the authorization (n° 457/18) of the Ethics Committee on Animal Experimentation, Federal University of Piauí/Brazilian. The BALB/c mice were housed in a standard holding room for laboratory animals under conditions of controlled temperature (22 $\pm 2°$C), humidity (45–65%), and artificial light (12:12-h light:dark cycle). Briefly, macrophages were removed three days after intraperitoneal administration of 3.0% thioglycolate by administering 8.0 mL of sterile phosphate-buffered saline (PBS, pH 7.4, 4°C) to the abdominal cavity. The cells were then added to sterile cell culture plates at the concentration of 1×10^5 cells per well in RPMI 1640 medium. The cell viability was evaluated over a concentration range of 0.04–2.50 mM, after incubation during 48 h. Afterward, the optical density was determined at 540 nm in a microplate reader ELx800 (BioTek Instruments, Winooski, VT). The concentration–response curve was plotted in order to determine the mean cytotoxic concentration (CC$_{50}$) for each agent.[16] All analysis and curves were performed using GraphPad$^®$ Prism version 6.00 (GraphPad$^®$ Software, San Diego, CA).

Hemolytic activity. Sheep blood erythrocytes were used for the evaluation of the hemolytic activity. A

suspension of 5.0% erythrocytes in 80 μL of PBS was mixed with increasing concentrations of CG-CuNPs or $CuSO_4 \cdot 5H_2O$ (0.16, 0.32, 0.64, 1.25, and 2.50 mM copper), reaching a final volume of 100 μL. After 1 h of incubation at 37°C, 200 μL of PBS was added to stop the reaction, and the mixture was then centrifuged at 1000*g* for 10 min. The supernatants were then collected and absorbance was measured at 540 nm in an ELISA plate reader. Positive controls (100% of hemolysis) and a negative control (0% of hemolysis) were used by replacement of CG-CuNPs or $CuSO_4 \cdot 5H_2O$ with an equal volume of distilled water or PBS, respectively.[9] All experiments were performed in triplicate.

Cell culture. 4T1 Luciferase (luciferase-expressing 4T1 mouse mammary tumor cell line) and NIH 3T3 cells (murine fibroblast cells) were routinely maintained in cell culture flasks (75 cm²) in an incubator (37°C, 5% CO_2 and 98% humidity) with DMEM cell culture medium containing 10% (v/v) fetal bovine serum (FBS), and 1% (v/v) antibiotic (100 IU/mL penicillin–100 μg/mL streptomycin) and passaged every three or four days. Trypsin–EDTA was added to the passaged cells to detach those which had adhered to the bottom of the flasks.

Cell viability assay. Cell viability was determined by MTT (Life Technologies, USA) assay in which 4T1 luciferase and NIH 3T3 cells were seeded on 96-well plates at a density of 5×10^3 cells and incubated at different concentrations 0.02–0.25 mM of CG-CuNPs at 37°C (5% CO_2).[17] Control groups corresponding to untreated cells, 4T1 luciferase and NIH 3T3 cells, or cells 4T1 luciferase and NIH 3T3 cells treated with acetic acid and ethanol at the same concentrations found in the formulations. The pH of the samples was adjusted to 7.4 with NaOH (10 M) whenever necessary. After treatments which lasted 24, 48, and 72 h, 15 μL MTT solution (5 mg mL^{-1} in PBS) was added to each well and incubation was carried out for 3 h at 37°C (5% CO_2). The culture medium was then aspirated and dimethyl sulfoxide 200 μL was added. The absorbance was monitored by a spectrophotometer with a microplate reader at a wavelength of 595 nm (SpectraMax®, model M2, Molecular Devices, USA).

Statistical analysis

OriginPro 8 was used to calculate the graph data from UV-Vis, DLS, DPV, FTIR, X-ray, and MTT for macrophages. Data from experiments of DLS, zeta potential, and AFM represent the mean value and standard deviation (mean ± SD) of values obtained from at least three independent experiments. Statistical differences between mean values of experimental data from MTT

(NIH 3T3 and 4T1 luciferase cells) were evaluated by two-way ANOVA, and pairwise comparisons were done by the Tukey test with *p* values of ≤0.05 were considered to be statistically significant (minimum $n = 3$), after analyses carried out in the GraphPad Prism 6.0 Software.

Results

Synthesis and characterization of copper NPs stabilized with CG

UV-vis spectra of CG-CuNPs (Figure 1) show the formation of NPs after reduction reaction over different times (24, 48, and 72 h). The intensity of this peak decreased over time, suggesting a loss of metallic particles after 24 h, probably due to oxidation. The CG-CuNPs showed an absorption peak from the surface plasmon at around 580 nm.[18] The intensity of the peak was maximal after 24 h, therefore all further experiments were carried out using NPs synthesized for 24 h.

The mean hydrodynamic diameter of the synthesized NPs measured by DLS (Figure 2) was 9.91 ± 5.31 nm. However, the DLS also showed CG-CuNPs of around 20–50 nm in a smaller quantity, which indicates the presence of small aggregates in solution, or a subpopulation of larger NPs. The zeta potential of the pure CG was also determined and presented a negative zeta potential around −3.73 ± 0.29 mV while CG-CuNPs shows more negative potential around −7.58 ± 0.50 mV.

DPV of the copper standard solution with different concentrations (1, 2, 4, 6, and 8 μM of Cu^{2+}) is shown in Figure 3(a). A strong positive linear correlation was found between the different concentrations
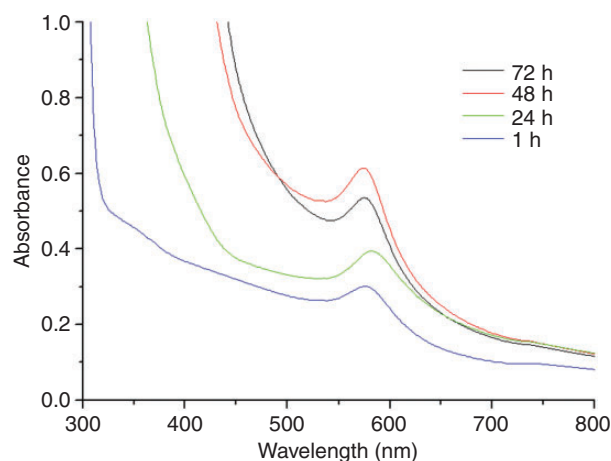

Figure 1. Absorption spectra of CG-CuNPs in suspension after 1, 24, 48, and 72 h of reduction.

($R^2 = 0.9927$, Figure 3(b)). The Cu^{2+} concentration in the CG-CuNP sample was calculated using the linear regression curve obtained (Figure 3(b)) and its value was 4.95 mM.

Figure 4 shows the FTIR spectra of the CG and CG-CuNPs. The CG spectrum shows transmissions at 3288 cm^{-1} that illustrate a stretching O-H vibration band, 2897 cm^{-1} from C–H stretching, 1612 cm^{-1} from O–H bending in the polymeric chain, 1371 cm^{-1} from CH bending, 1124, 1066, and 1011 cm^{-1} due to C–O–C stretching from glycosidic bonds and O–H bending of alcohols.[6,19] Many of the same bands were observed in the CG-CuNPs. A shift in the peak from 1704 cm^{-1} is observed after the stabilization of CG-CuNPs (Figure 4) which is characteristic of C=O stretching vibration of glucuronic acid present in this polysaccharide.[20]

The phases of the samples were determined by XRD analysis by searching against databases. In Figure 5, it is possible to observe peaks at $2\theta = 8.86°$, $15.34°$, and $17.76°$ in the CG-CuNPs spectrum which are also seen in $CuSO_4$ (Inorganic Crystal Structure Database).[21]
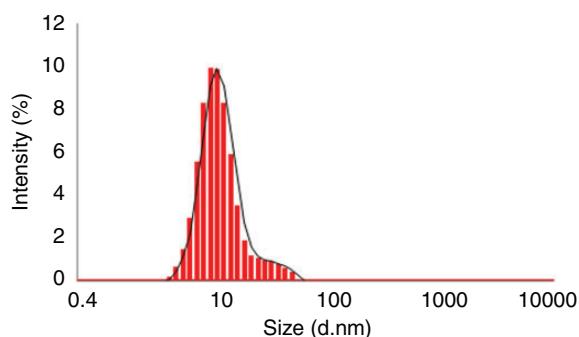
CG, used as a stabilizer, presented a broad peak around $2\theta = 23°$ because of the characteristic highly amorphous nature of this polymer.[22,23] Meanwhile, ascorbic acid showed peaks at $2\theta = 12.08°$ and $13.44°$ in accordance with data from the Cambridge Structural Database.[24]

Morphological characterization of the CG-CuNPs was made by AFM, some results are illustrated in Figure 6. The mean size of particles measured by AFM technique was equal to 19.89 ± 9.32 nm.

Microbiological assay

The minimum inhibitory concentration (MIC) is that capable of preventing the growth of 99.9% of the bacterial inoculum used (10^5 CFU/mL), whereas the MBC is that which kills the microorganisms. The results of antibacterial assays (MIC and MBC) CG-CuNPs against Gram-positive bacteria are summarized in
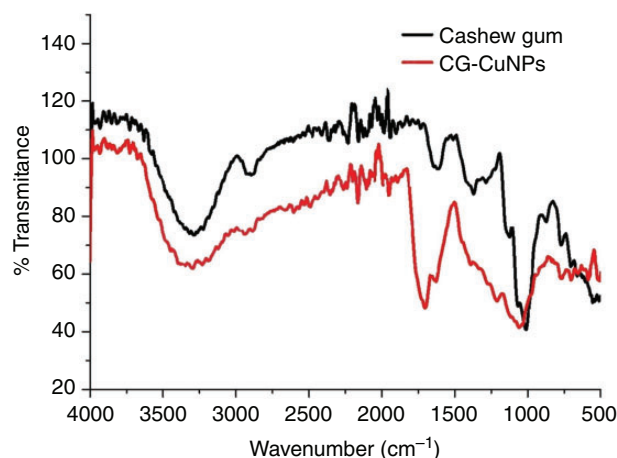

Figure 2. Particle size distribution of CG-CuNPs by DLS.

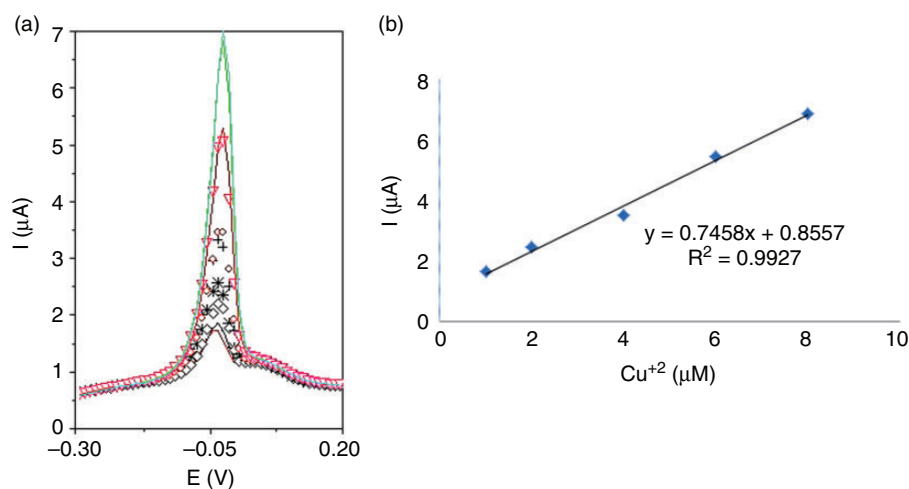**Figure 4.** ATR-FTIR spectra of cashew gum and CG-CuNPs.

Figure 3. Differential pulse voltammogram (a) for different concentrations of Cu^{2+} and the derived linear regression curve (b).

Table 1. CG-CuNPs presented MIC and MBC of 0.64 mM that was lower than the $CuSO_4 \cdot 5H_2O$ concentration, equal to 2.50 mM, showing that the NPs is more active against Gram-positive strain, *S. aureus* ATCC 29213. The synthesized NPs showed a bactericidal effect, since the MIC was equal to MBC, that is, the concentration that inhibits bacterial growth is the same as to effectively kill the bacterium used.[25] Thus such results indicated that the copper NPs can be used as an alternative strategy against bacterial contamination as a potential new antimicrobial agent.
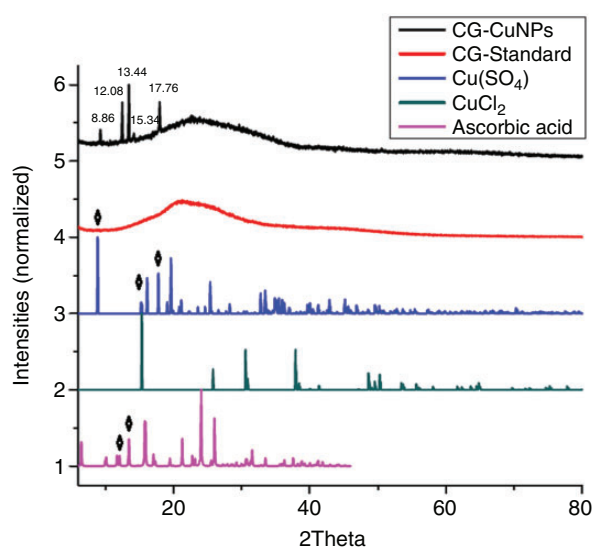

Figure 5. X-ray diffractogram of CG-CuNPs, CG-Standard, $CuSO_4 \cdot 5H_2O$, $CuCl_2$, and ascorbic acid.

Cytotoxicity assessment

MTT assay. The CC_{50} values (Figure 7) were determined for both CuNPs (0.1868 mM; confidence intervals: 0.1204–0.2898 mM) and $CuSO_4 \cdot 5H_2O$ (0.1809 mM; confidence intervals: 0.1649–0.1985 mM). Any significant difference was observed between the respective CC_{50} values, due to both CG-CuNPs and $CuSO_4 \cdot 5H_2O$ promoted an equipotent concentration-dependent reduction in macrophages viability from 0.04 to 0.16 mM. On the other hand, the cell viability for CG-CuNPs at concentrations of 0.32 and 0.64 mM was respectively 1.8- or 1.7-fold higher than $CuSO_4 \cdot 5H_2O$ at same concentrations. Thus, less cytotoxicity was observed for CG-CuNPs at these concentrations, which were the same observed for MIC and MBC in antibacterial assays (Table 1). Besides, no hemolytic effect for CG-CuNPs or $CuSO_4 \cdot 5H_2O$ was observed on sheep blood erythrocytes even at the highest concentration of 2.50 mM (data not shown). Thus, these results suggest a potential minor cytotoxic effect

Table 1. Minimum inhibitory concentration (MIC) and minimum bactericidal concentration (MBC) of CG-CuNPs suspension against reference strain standard of *Staphylococcus aureus* (ATCC 29213) in comparison to copper sulfate solution.

Sample	MIC (mM)	MBC (mM)
CG-CuNPs	0.64	0.64
$CuSO_4 \cdot 5H_2O$	2.50	2.50

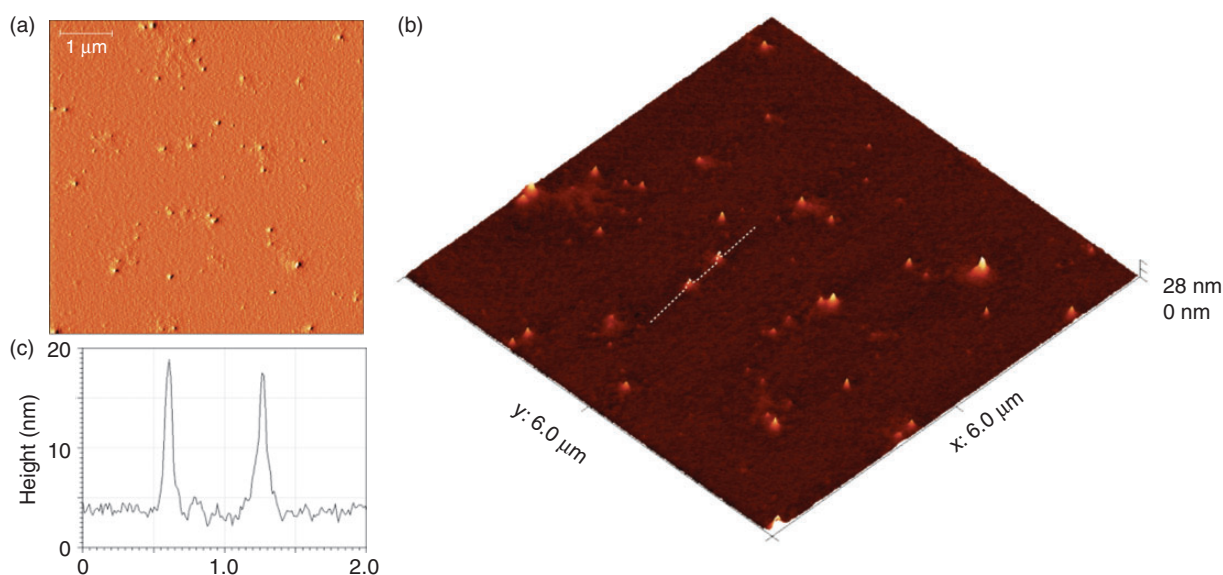CG: cashew gum; MBC: Minimal bactericidal concentration; MIC: minimal inhibitory concentration.

Figure 6. AFM images of CG-CuNPs after air drying on the mica at room temperature. (a) Amplitude image; (b) height image rendered in 3D; (c) height profile through two nanoparticles. The location of this profile is indicated by the dotted line in (b).
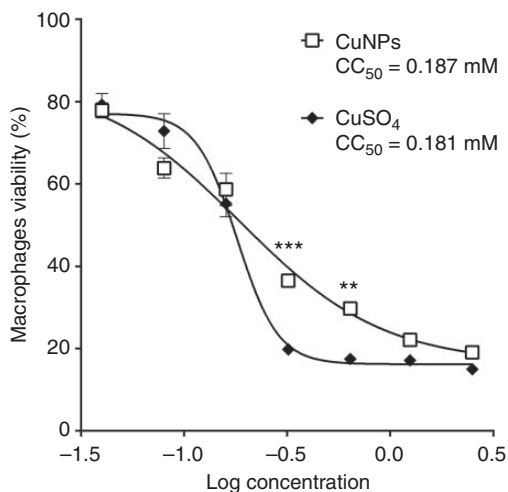
Figure 7. Cytotoxicity of CG-CuNps and CuSO$_4$·5H$_2$O on BALB/c mice peritoneal macrophages. The graph represents the mean cell viability (%) $\pm$ SEM of experiments carried out in triplicate. **$p < 0.001$ when compared with control; ***$p < 0.001$ when compared with the respective concentration of CG-CuNPs and CuSO$_4$·5H$_2$O. For the experiment a cashew gum (CG) 0.25% control was performed with the mean cell viability $98 \pm 2\%$.

for CG-CuNPs at concentrations that are able to promote antibacterial activity.

Cell viability. The analyses of the effect of CG-CuNPs on the viability of 4T1 luciferase (4T1 LUC) and NIH 3T3 cells (murine fibroblast cells) within a 24-, 48-, and 72-h period are shown in Figure 8. The 4T1 LUC cell used is syngeneic breast cancer model because the 4T1 cell line is derived from a spontaneously arising BALB/c mammary tumor and because having metastatic properties extensively characterized. In addition, its applications are used for investigation on determination of effects of drugs and of the therapeutic procedures on breast tumor growth, its metastasis and on the drug's efficacy and toxicity studies on these cells.[26] While NIH 3T3 is a cell line used to a suitable transfection of host and this cell line is highly sensitive to sarcoma virus focus formation and leukemia virus propagation and has proved to be very useful in DNA transfection studies.[27]

Control experiments were conducted to evaluate the toxicity of the delivery system without CG-CuNPs at 24-, 48-, and 72-h period. The control samples did not
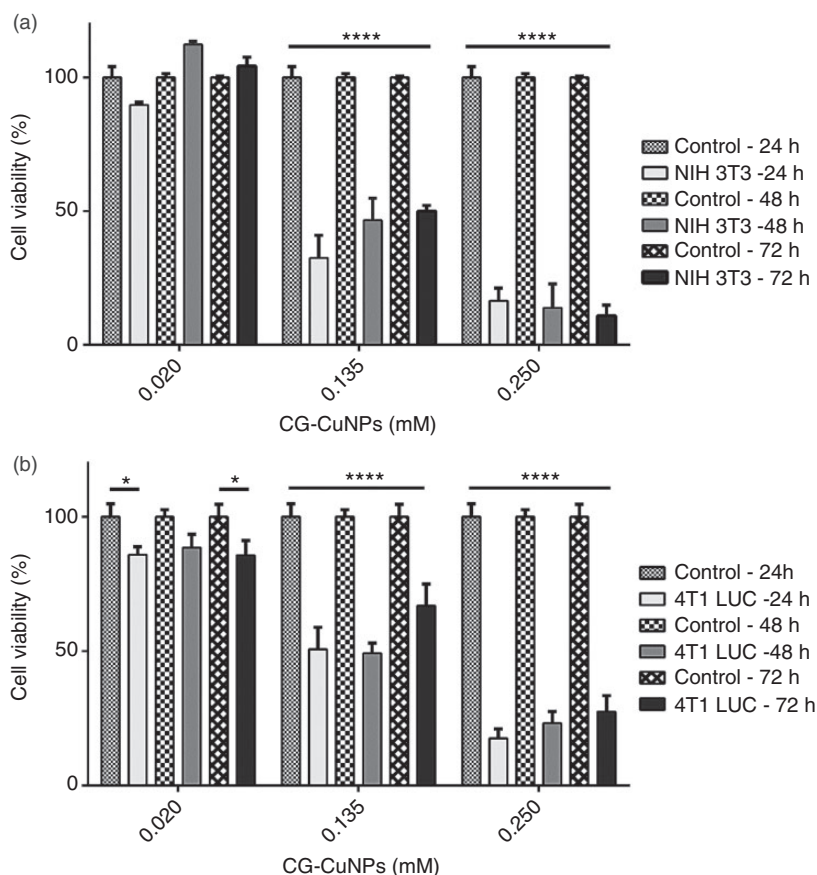

Figure 8. Mean cell viability (%) $\pm$ SD from NIH 3T3 (a) and 4T1 LUC (b) cells against CG-CuNPs 0.020, 0.135 and 0.250 mM for 24, 48, and 72 h. All the experiments were carried out in triplicate to *$p < 0.05$ or ****$p < 0.001$ when compared with control. For the experiment a cashew gum (CG) 0.25% control was performed with the mean cell viability $97 \pm 3\%$ for NIH 3T3 and $95 \pm 4\%$ for 4T1 LUC. All concentrations refer to concentration of copper.

affect cell viability and toxicity was not observed. The presence of 0.135 mM of CG-CuNPs significantly reduced in the cell viability of both cells, 4T1 LUC and NIH 3T3 cells (49.3% and 67.5%, respectively; $p < 0.0001$) after only 24 h, by comparison with the control group, while the lowest concentration (0.020 mM) significantly decreased ($p < 0.05$) only the viability of the 4T1 LUC tumor cell line (Figure 8(b)). The use of in vitro cytotoxicity tests involving cell viability assays is the first step in the evaluation of the biocompatibility of a substance.[27]

Concentrations of 0.250 mM CG-CuNPs were found to decrease NIH 3T3 and 4T1 LUC cell viability by 89.1% and 72.5% ($p < 0.001$), respectively, by comparison with the control group in both cells in 72 h periods. As shown in Figure 8(a), significant reduction in cell viability for 4T1 LUC with increase of the CG-CuNPs concentration is observed in all periods.

Discussion

CG is a natural polymer that due to its characteristic glycosylation can be chemically modified in order to improve the properties for chosen applications. CG has been applied as stabilizer of carbohydrates-based polymeric nanoparticles, and for controlled release of bioactive substances in the materials area. [8,13] CG, as a natural polymer, is interesting due to low toxicity, biodegradability, stability, and biocompatibility as compared to synthetic polymers.[28]

Metal NP chemistry is a domain in rapid expansion and their most useful optical properties rely on a strong absorption in the visible spectrum, called the surface plasmon band.[29] However, there are many issues with metal NP synthesis: the stability of NPs, aggregation of NPs, control of crystal growth, morphology, size and size distribution, extraction, and purification of produced NPs for further applications.[30]

Characterization by UV-visible technique confirmed the reduction of copper ions to CG-CuNPs. Copper NPs stabilized with gum Kondagogu displayed an absorption peak at around 558 nm after reduction process and this peak was assigned to these NPs.[29]

The size of dispersed nanoparticles measured by DLS together with domain size estimated from the AFM showed small NPs. The negative Zeta potential of pure CG is due to the presence of some carboxylic acid groups in the carboxylate form (COO-) in its structure [8], proving the anionic nature of CG.[31].

The FTIR spectra of NPs can indicate the presence of chemical bonds and molecular structures that can be important in the formation[32] of copper NPs. The FTIR spectra confirmed that the copper NPs were stabilized with CG, via changes that affected the stretching vibration of the carboxylic acid bond of the glucuronic acid[33] at 1704 cm^{-1}.

The identification of copper crystallographic phases CG-CuNPs is particularly difficult. The 2θ data showed two peaks derived from copper NPs, formed from $CuSO_4 \cdot 5H_2O$ in this reduction process, as well as indicating a relatively low purity and crystallinity of the final product. The peak from CG suggests that this polymer has an action as coating agent[28] since x-ray data showed there is gum coating on the surface of the copper NPs. However, a stability study of these NPs would be necessary to confirm this.

The results of AFM and UV-vis showed that the chemical reduction process induced the formation of small NPs.[33,34] In addition to the small, approximately quasi-spherical particles, many amorphous materials distributed on the surface were found by AFM, presumably corresponding to CG not directly linked to the particles.

The fact that this material is separate from the particles may indicate the presence of loose material in solution. However, a drying artifact cannot be ruled out. Comparison with the DLS results in "Microbiological assay" section would seem to suggest that most of the polymers are connected to the particles in solution since only one major peak was observed in the DLS. It is notable that the diameter from AFM is approximately twice as large as the result obtained by DLS. This may indicate that the model used by the DLS to estimate hydrodynamic diameter is inadequate for these samples. The model assumes a solid sphere moving in solution, whereas in our case, we probably have solid copper sphere surrounded by a looser gum coating. On the other hand, the DLS probes many more particles than the AFM, so the AFM results may represent statistical outliers.

Copper NPs synthesized by Kruk et al.[18] also showed activity against *S. aureus*, corroborating with our findings (Table 1). Published data indicate stronger antimicrobial activity of copper NPs against Gram-positive bacteria when compared with the Gram-negative bacteria.[32,35]

One of the hypotheses that have been proposed to explain the mechanism of antimicrobial activity of metals NPs is its incorporation on the cell membrane, which causes leakage of intracellular substances and eventually causes cell death.[18]

Another mechanism has been proposed to interpret the antibacterial behavior of copper NPs that could be attributed to the generation of reactive oxygen species that are responsible for damaging the cell membrane of Gram-negative bacteria, as well as Gram-positive bacteria that have thicker peptidoglycan cell membranes when compared with the Gram-negative bacteria. In addition, CuNPs are able to change the membrane

electrochemical potential and promote DNA damage after interaction with these structures.[36,37] The mechanisms above mentioned are characteristic of antimicrobial agents with bactericidal effect, such as the NPs synthesized in this study.

The assessment of cell viability over all periods at the 0.020, 0.135, and 0.250 mM concentrations of CG-CuNPs presented significant inhibition of the growth of 4T1 LUC cells by comparison with the control group (Figure 8(b)). Likewise, we observed that after 24, 48, and 72 h there was significant decrease in viability of NIH 3T3 treated with CG-CuNPs at 0.135 and 0.250 mM copper concentrations by comparison with the control group ($p < 0.001$). Therefore, CG-CuNPs inhibited the growth of the 4T1 LUC and NIH 3T3 cells in a concentration-dependent but not time-dependent manner, at concentrations below that caused hemolysis (0.32 and 0.64 mM).

The cytotoxic effect of copper NPs was observed in studies by Triboulet et al., wherein was reported CuO NPs contributed to the inflammatory processes of the central nervous system. In addition, CuO NPs can induce toxicity (at 125 µM) or to interfere with some essential macrophage functions due to perturbation of the cellular survival functions.[4]

Conclusion

This work showed that copper NPs were formed by the chemical reduction of the $CuSO_4 \cdot 5H_2O$ salt and illustrate a simple and effective route to an aqueous suspension of CG-CuNPs with antimicrobial activity. The size obtained for copper NPs was controlled by the presence of ascorbic acid and sodium borohydride. The average size of NPs was about 10 nm. Antimicrobial tests demonstrated that CG-CuNPs were active against the Gram-positive bacteria *S. aureus* ATCC 29213, in addition, CG-CuNPs are more active than free copper, which makes NPs more effective as an antibacterial agent. Cell viability assays indicated that the NPs inhibited the growth of 4T1 LUC and NIH 3T3 cells at a copper concentration (0.250 mM) less than the concentration found to induce hemolysis over a 24-h period. Therefore, copper NPs stabilized by CG can be used as an antimicrobial agent with lower cytotoxic effects than its $CuSO_4 \cdot 5H_2O$ precursor.

Declaration of Conflicting Interests

The author(s) declared no potential conflicts of interest with respect to the research, authorship, and/or publication of this article.

ORCID iD

Daniel Dias Rufino Arcanjo https://orcid.org/0000-0001-7021-2744

References

1. Chandra S, Kumar A and Tomar PK. Synthesis and characterization of copper nanoparticles by reducing agent. *J Saudi Chem Soc* 2014; 18: 149–153.
2. Bogdanović U, Lazić V, Vodnik V, et al. Copper nanoparticles with high antimicrobial activity. *Mater Lett* 2014; 128: 75–78.
3. Ruparelia JP, Chatterjee AK, Duttagupta SP, et al. Strain specificity in antimicrobial activity of silver and copper nanoparticles. *Acta Biomater* 2008; 4: 707–716.
4. Triboulet S, Aude-Garcia C, Armand L, et al. Comparative proteomic analysis of the molecular responses of mouse macrophages to titanium dioxide and copper oxide nanoparticles unravels some toxic mechanisms for copper oxide nanoparticles in macrophages. *PLoS One* 2015, 10: e0124496. DOI: 10.1371/journal.pone.0124496
5. Carvalho NS, Silva MM, Silva RO, et al. Gastroprotective properties of cashew gum, a complex heteropolysaccharide of *Anacardium occidentale*, in naproxen-induced gastrointestinal damage in rats. *Drug Dev Res* 2015; 76: 143–151.
6. Pitombeira NAO, Veras Neto JG, Silva DA, et al. Effect of chemical modification on the solubility and swelling of microspheres based on carboxymethyl cashew gum and chitosan. *Carbohydr Polym* 2015; 117: 610–615.
7. Oliveira LGC, Brito LM, Alves MMM, et al. *In Vitro* effects of the neolignan 2,3-dihydrobenzofuran against *Leishmania amazonensis*. *Basic Clin Pharmacol Toxicol* 2017; 120: 52–58.

8. Paula HCB, Rodrigues MLL, Ribeiro WLC, et al. Protective effect of cashew gum nanoparticles on natural larvicide from *Moringa oleifera* seeds. *J Appl Polym Sci* 2012; 124: 1778–1784.

9. Moore TL, Rodriguez-Lorenzo L, Hirsch V, et al. Nanoparticle colloidal stability in cell culture media and impact on cellular interactions. *Chem Soc Rev* 2015; 44: 6287–6305.

10. Napper DH. *Polymeric stabilization of colloidal dispersions*. London: Academic Press, 1983.

11. CDC Antibiotic/antimicrobial resistance, https://www.cdc.gov/drugresistance/index.html (2018, accessed 10 September 2018).

12. WHO Latest global cancer data, https://www.who.int/cancer/PRGlobocanFinal.pdf (2018, accessed 2 September 2018).

13. Castro RAO, Monte RS, Mendes LG, et al. Electrosynthesis and characterization of polypyrrole/cashew gum composite grown on gold surface in aqueous medium. *Int J Electrochem Sci* 2017; 12: 50–61.

14. CLSI – Clinical Laboratory Standards Institute. Approved standard M07-A10. Wayne, PA, 2015.

15. Rodrigues KAF, Amorim LV, Dias CN, et al. *Syzygium cumini* (L.) skeels essential oil and its major constituent α-pinene exhibit anti-*Leishmania* activity through immunomodulation *in vitro*. *J Ethnopharmacol* 2015; 55: 32–40.

16. Reilly TP, Bellevue IIF, Woster PM, et al. Comparison of the *in vitro* cytotoxicity of hydroxylamine metabolites of sulfamethoxazole and dapsone. *Biochem Pharmacol* 1998; 55: 803–810.

17. Jardim KV, Joanitti GA, Azevedo RB, et al. Physicochemical characterization and cytotoxicity evaluation of curcumin loaded in chitosan/chondroitin sulfate nanoparticles. *Mater Sci Eng C* 2015; 56: 294–204.

18. Kruk T, Szczepanowicz K, Stefańska J, et al. Synthesis and antimicrobial activity of monodisperse copper nanoparticles. *Colloids Surf B Biointerfaces* 2015; 128: 17–22.

19. Umer A, Naveed S, Ramzan N, et al. A green method for the synthesis of copper nanoparticles using L-ascorbic acid. *Matéria* 2014; 19: 197–103.

20. Silva DA, Feitosa JPA, Maciel JS, et al. Characterization of crosslinked cashew gum derivatives. *Carbohydr Polym* 2006; 66: 16–26.

21. Hu C, Li P, Zhang W, et al. Effect of cupric salts ($Cu(NO_3)_2$, $CuSO_4$, $Cu(CH_3COO)_2$) on $Cu_2(OH)PO_4$ morphology for photocatalytic degradation of 2,4-dichlorophenol under near-infrared light irradiation. *Mater Res* 2017; 20: 407–412.

22. Oliveira EF, Paula HCB and Paula RCM. Alginate/cashew gum nanoparticles for essential oil encapsulation. *Colloids Surf B Biointerfaces* 2014; 113: 146–151.

23. Ramesan MT and Surya K. Fabrication and characterization of biopolymer nanocomposites from natural resource materials. *Polym Compos* 2017; 38: E66–E73.

24. Crystallography Resources: Cambridge Structural Database and Inorganic Crystal Structure Database, https://ucsd.libguides.com/crystallography (2018, accessed 30 June 2018).

25. Levison ME and Levison JH. Pharmacokinetics and pharmacodynamics of antibacterial agents. *Infect Dis Clin North Am* 2009; 23: 791–815.

26. Wood LM, Pan Z-K, Seavey MM, et al. The ubiquitin-like protein, ISG15, is a novel tumor-associated antigen for cancer immunotherapy. *Cancer Immunol Immunother* 2012; 61: 689–700.

27. Bergfeld SA, Blavier L and DeClerck YA. Bone marrow-derived mesenchymal stromal cells promote survival and drug resistance in tumor cells. *Mol Cancer Ther* 2014; 13: 962–975.

28. Kumar A, Moin A, Shruthi R, et al. Cashew gum a versatile hydrophyllic polymer: a review. *CDTH* 2012; 7: 2–12.

29. Suresh Y, Annapurna S, Singh AK, et al. Characterization of Kondagogu stabilized copper nanoparticles and their surface enhanced Raman scattering studies. *Int J Nanomater Biostruct* 2014; 4: 35–40.

30. Iravani S, Korbekandi H, Mirmohammadi SV, et al. Synthesis of silver nanoparticles: chemical, physical and biological methods. *Res Pharm Sci* 2014; 9: 385–406.

31. Leite AJ, Costa RR, Costa AMS, et al. The potential of cashew gum functionalization as building blocks for layer-by-layer films. *Carbohydr Polym* 2017; 174: 849–885.

32. Rasool U and Hemalatha S. Marine endophytic actinomycetes assisted synthesis of copper nanoparticles (CuNPs): characterization and antibacterial efficacy against human pathogens. *Mater Lett* 2017; 194: 176–180.

33. Al-Shalalfeh MM, Onawole AT, Saleh TA, et al. Spherical silver nanoparticles as substrates in surface-enhanced Raman spectroscopy for enhanced characterization of ketoconazole. *Mater Sci Eng C* 2017; 76: 356–364.

34. Wu J, Xiang D and Gordon R. Monitoring gold nanoparticle growth in situ via the acoustic vibrations probed by four-wave mixing. *Anal Chem* 2017; 89: 2196–2200.

35. Shankar S and Rhim J-W. Effect of copper salts and reducing agents on characteristics and antimicrobial activity of copper nanoparticles. *Mater Lett* 2014; 132: 307–311.

36. Padil VVT and Černík M. Green synthesis of copper oxide nanoparticles using gum karaya as a biotemplate and their antibacterial application. *Int J Nanomed* 2013; 8: 889–898.

37. Din MI, Arshad F, Hussain Z, et al. Green adeptness in the synthesis and stabilization of copper nanoparticles: catalytic, antibacterial, cytotoxicity, and antioxidant activities. *Nanoscale Res Lett* 2017; 12: 638.